Dalton Transactions RSCPublishing

ARTICLE

Comparative synthetic, magnetic and theoretical study of functional M_4Cl_4 cubane-type Co(II) and Ni(II) complexes

Cite this: DOI: 10.1039/x0xx00000x

Received 00th January 2012,
Accepted 00th January 2012

DOI: 10.1039/x0xx00000x

www.rsc.org/

Alessio Ghisolfi,[a] Kirill Yu. Monakhov,[b]* Roberto Pattacini,[a] Pierre Braunstein,[a]* Xavier López,[c] Coen de Graaf,[c,d] Manfred Speldrich,[b] Jan van Leusen,[b] Helmut Schilder,[b] and Paul Kögerler[b,e]*

We describe the synthesis, structures, and magnetochemistry of the new M_4Cl_4 cubane-type cobalt(II) and nickel(II) complexes with formula $[M(\mu_3\text{-}Cl)Cl(\mathbf{HL{\cdot}S})]_4$ (**1**: M = Co and **2**: M = Ni) where **HL·S** represents a pyridyl-alcohol-type ligand with a thioether functional group. The solid-state structures of **1** and **2** were determined by X-ray crystallography. Dc and ac magnetic susceptibility measurements of **1** and **2** were modeled with the computational framework CONDON 2.0. Although both complexes **1** and **2** are *iso*structural, with each of their transition metal ions in a pseudo-octahedral coordination environment of four Cl atoms and N,O-donor atoms of one chelating **HL·S** ligand, they show dissimilar magnetic behaviour due to substantially different ligand field effects of Co(II) in **1** and Ni(II) in **2**. Magnetochemical measurements show that compound **1** possesses a low-spin ground state (S_{LS} = 0) and an averaged antiferromagnetic coupling characterised by J = –0.14 cm^{-1}, whilst **2** is characterised by an intermediate ground state (S_{IS} = 2) and experiences a ferromagnetic coupling (J = +10.6 cm^{-1}). In contrast to **1**, compound **2** is postulated to be a single-molecule magnet (SMM) and is of great interest for future surface deposition studies. A computational analysis based on density functional theory (DFT) was performed to explore possible magnetostructural correlations in these compounds. Using a two-J model Hamiltonian, it revealed that compound **1** has four positive and two (small) negative $J_{Co\text{-}Co}$ isotropic interactions leading to a S_{HS} = 6 ground state. Taking into account the magnetic anisotropy one would recover a M_S = 0 ground state since D > 0 from computations. In **2**, all the J constants are positive and, in this framework, the zero-field splitting energy parameter characterising the axial anisotropy was estimated to be negative (D = –0.44 cm^{-1}). The computational results are consistent with compound **2** being a SMM.

Introduction

In the course of studies originally devoted to the development of new homogeneous Ni(II) pre-catalysts for ethylene oligomerisation,[1] we have reported in recent years on the synthesis, structures and magnetism of cubane-, *pseudo*-cubane-, and wheel-shaped complexes formed in the reactions between chelating pyridyl-alcohol/-ate ligands and Ni(II) precursors.[2] For comparison, extensions to the assembling of Co(II) ions using the same N,O ligands were performed.[3] In view of the interesting magnetic properties[4] displayed by some of the complexes isolated, including the slow relaxation of their magnetisation, we considered the possibility to functionalise such structurally well-defined molecules by electron donating groups in order to assist their subsequent adsorption on a metal surface (substrate). Surface-grafted molecules[5] with magnetic responses are indeed of high current interest in the area of spin transport electronics that interfaces synthetic chemistry with molecular magnetism[6] and condensed matter physics.

Although thiol (–SH) groups exhibit a high affinity for gold, thus allowing the covalent binding of molecules to a substrate or offering a well-defined conductance of a single-molecule junction between two Au electrodes,[7] their air-sensitivity may limit the application of thiol-containing metal complexes. In contrast, thioether functions are air-stable and also allow molecular anchoring to surfaces.[8] We thus aimed at the synthesis of a new polytopic multidentate ligand that contains a pendant thioether group along with N,O-donor groups shown previously to provide effective chelation of metal ions in coordination clusters. As a result, we describe here the

synthesis and structural chemistry of open-shell cubane-type cobalt(II) (**1**) and nickel(II) (**2**) complexes resulting from the coordination of a new tridentate pyridyl-alcohol-type ligand to Co(II) and Ni(II) centres. Being decorated at their periphery with thioether functions,[9] the *iso*structural compounds [M(μ_3-Cl)Cl(**HL·S**)]$_4$ (**1**: M = Co and **2**: M = Ni) provide an ideal basis for a detailed comparative experimental and computational analysis of their molecular magnetic characteristics and have led to a clear-cut understanding of their similarities and differences. Thus, we discuss herein the results of dc and ac magnetic susceptibility measurements, of magnetochemical modelling with our computational framework CONDON 2.0 for molecular spin structures,[10] and of *broken-symmetry* density functional theory[11] (DFT) calculations. Note that although cubane-type structures are numerous in the inorganic chemistry of the transition metals, a direct comparison between the magnetic properties of two *iso*structural complexes is rather rare, despite its great fundamental interest since the spin exchange interactions in metal complexes are usually very sensitive to the ligand-field effects.

Results and discussion

Synthesis of the complexes and description of their crystal structures

To increase the coordination versatility of the pyridyl-alcohol ligands used in previous studies on polynuclear open-shell transition metal compounds,[2,3] we designed a tridentate ligand comprising the donor atoms N, O, and S. The new, brown 4-(pyridin-2-ylmethyl)tetrahydro-2*H*-thiopyran-4-ol ligand [hereafter referred to as **HL·S**] with amino-alcohol and dialkyl sulphide (or thioether) functional groups was synthesised in good yield (73%) by reaction of lithiated 2-picoline with tetrahydro-4H-thiopyran-4-one in THF (Scheme 1).

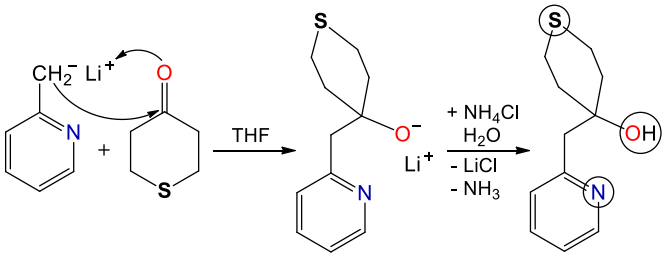

Scheme 1. Synthesis of the tridentate **HL·S** ligand (right) from lithiated 2-picoline (left) and tetrahydro-4H-thiopyran-4-one (middle).

The reaction of one equiv. of the **HL·S** ligand with one equiv. of $CoCl_2$ or [$NiCl_2$(dme)] (dme = dimethoxyethane) in THF at room temperature afforded tetranuclear cubanes: the blue Co(II) complex [Co(μ_3-Cl)Cl(**HL·S**)]$_4$ (**1**) and the yellow Ni(II) complex [Ni(μ_3-Cl)Cl(**HL·S**)]$_4$ (**2**), in *ca.* 63% and 74% yield, respectively (Scheme 2). According to thermogravimetric analyses (TGA), **2** exhibits higher thermal stability against degradation under N_2 than **1**. The crystallinity of **1** and **2** was retained upon heating to 210 °C and 250 °C, respectively. Broad signals in the ^{1}H and ^{13}C NMR spectra of **1** and **2** pointed to the magnetic nature of these complexes.

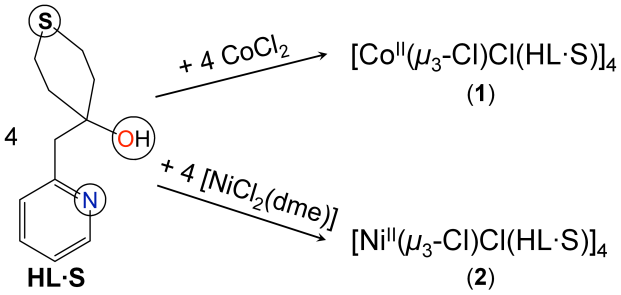

Scheme 2. Synthesis of the tetranuclear Co(II) and Ni(II) complexes with the general formula [M(μ_3-Cl)Cl(**HL·S**)]$_4$ (**1**: M = Co; **2**: M = Ni).

The solid-state molecular structures of **1** and **2** were revealed by single crystal X-ray diffraction analyses. **1** and **2** crystallise in the tetragonal space group $I4_1/a$ (Table S1, Supporting Information), have crystallographically imposed S_4 symmetry and display cubane-like {M$_4$(μ_3-Cl)$_4$} core structures composed of four mononuclear [MCl_2(**HL·S**)] formula isomers each (Figure 1).[12]

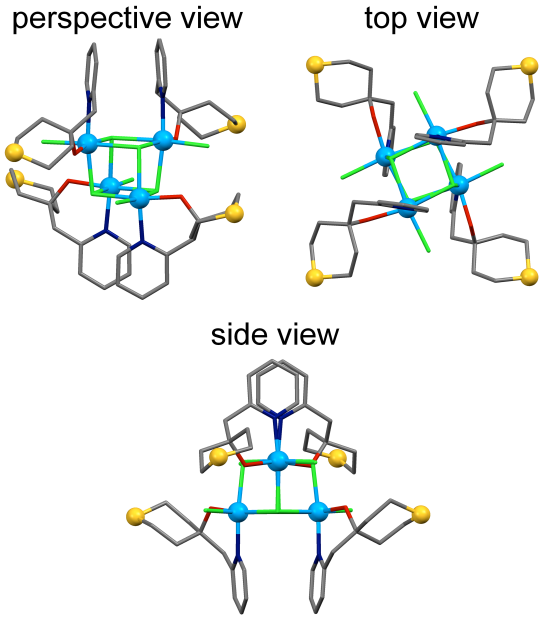

Fig. 1. Different views of the solid-state structures of **1** and **2**. Hydrogen atoms are omitted for clarity. Colour code: C, dark-grey; N, dark-blue; O, red; S; yellow; Cl, light-green; M, light-blue (**1**: M = Co; **2**: M = Ni). The metal and sulphur atoms are represented as ball-and-stick models.

Each metal centre in the *iso*structural complexes **1** and **2** is coordinated by one terminal Cl atom, three triply-bridging μ_3-Cl atoms, and one chelating **HL·S** ligand through the N,O-donor atoms. Alternatively, these structures can be viewed as formed by two interpenetrating Ni$_4$ and Cl$_4$ tetrahedra. The S atoms in the tail of the **HL·S** chelate are not involved in any coordination bond (Figure 1); no specific structural influence of

the thioether functions was thus identified at this stage. The Co^{2+} and Ni^{2+} ions in the representative structures are in local pseudo-octahedral environments, with the metal–element bonds in the {$CoCl_4NO$} fragments being slightly elongated when compared with those in the {$NiCl_4NO$} ones (Figure 2).

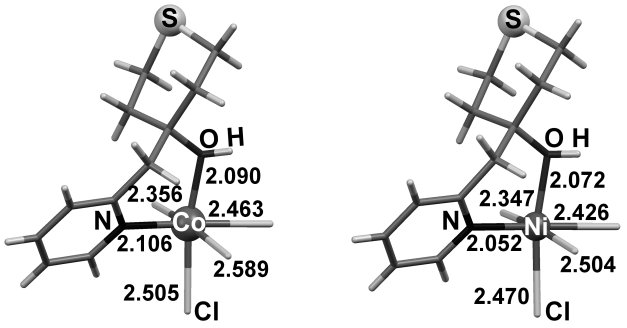

Fig. 2. Pseudo-octahedral coordination geometry of the Co(II) and Ni(II) ions constitutive of **1** and **2**, respectively. Relevant bond lengths (Å) are shown and more details are provided in the caption to Figure 3.

There are four shorter (**1**: $d_{Co\cdots Co}$ = 3.6804(5) Å; **2**: $d_{Ni\cdots Ni}$ = 3.6029(6) Å) and two longer (**1**: $d_{Co\cdots Co}$ = 3.8559(5) Å; **2**: $d_{Ni\cdots Ni}$ = 3.7378(6) Å) sets of non-bonding metal···metal separations in **1** and **2**. As a result, the central {$Ni_4(\mu_3\text{-}Cl)_4$} cubane core of **2** is somewhat contracted with respect to the {$Co_4(\mu_3\text{-}Cl)_4$} core of **1**. This complies well with the differences between the crystal radii (Σr_{cryst}) and the effective ionic radii (Σr_{ion}) of the hexa-coordinate Co and Ni dications (Σr_{cryst}: 0.89 Å for high-spin Co^{2+} and 0.83 Å for Ni^{2+}; Σr_{ion}: 0.75 Å for high-spin Co^{2+} and 0.69 Å for Ni^{2+})[13] or the covalent radii (Σr_{cov}) of the Co and Ni atoms (Σr_{cov}: 1.50 Å for high-spin Co and 1.24 Å for Ni).[14] The magnetic relevant M–μ_3-Cl–M bond angles fall in the ranges 93.48(2) – 98.38(2)° for **1** (M = Co) and 93.88(3) – 97.43(3)° for **2** (M = Ni) and are slightly larger than the 90° angles for a regular cube.

Cubane-like structures with cobalt[15] and nickel[2,16] ions are not scarce and they generally feature the {$M_4(\mu_3\text{-}O_4)$} cubane cores. The first Co(II) SMM, $[Co(hmp)(MeOH)Cl]_4$ (hmp^- = 2-hydroxymethylpyridine), was reported in 2002[17] and the first Ni(II) SMMs, $[Ni(hmp)(ROH)Cl]_4$ (R = Me, CH_2Me, $CH_2CH_2CMe_3$), in 2003.[18] Despite the various ligand systems that have been used to form cubane-type Co(II) and Ni(II) complexes, **1** and **2** belong to the rare family of compounds with the general formula $[M(II)X_2Z_2]_4$ where M is a transition metal, X is a halogen, and *Z* a two electron donor ligand.[2c,19] Thus, **1** represents the first cubane complex having the core vertices occupied by four Co(II) centres and four μ_3-capping halides (X = Cl) and **2** is a rare representative of the family of compounds displaying a {$Ni_4(\mu_3\text{-}X_4)$} cubane core (X = F, Cl).[2c,16h,y] Their magnetochemistry is not yet fully understood.

Another feature shared by complexes **1** and **2** is the intramolecular O–H···Cl non-classical hydrogen bonding[2c,16j,l] illustrated in Figure 3. Each of the four terminal Cl atoms in **1** and **2** is involved in such a bonding to the closest H atom from the OH functional group of the **HL·S** ligand. The resulting multiple O–H···Cl interactions, fully identical in each cluster ($d_{O\cdots Cl}$ = 3.233(2) Å in **1** and 3.206(3) Å in **2**), are likely to substantially contribute to the stability of these cubane-like structures. An additional source of stabilisation involved in the self-aggregation of the mononuclear $[MCl_2(\mathbf{HL{\cdot}S})]$ complexes toward the formation of **1** or **2** may be the intramolecular π-π stacking interactions between crystallographically pairwise parallel pyridyl (Py) fragments of the **HL·S** ligands (Figure 1). The intramolecular distances between the geometrical centres of these Py rings are $d\pi_{Py}\cdots\pi_{Py}$ = 3.770(2) Å in **1** and 3.757(2) Å in **2**.

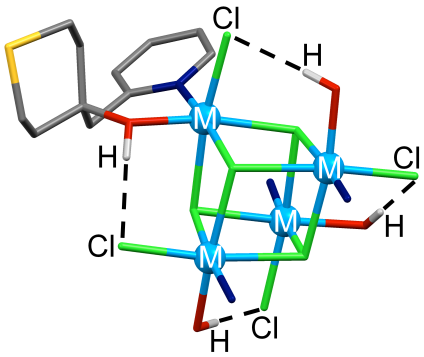

Fig. 3. Weak intramolecular O–H···Cl interactions in the [M(μ_3-Cl)Cl(**HL·S**)]$_4$ complexes (**1**: M = Co; **2**: M = Ni). Only one **HL·S** ligand is explicitly depicted. Hydrogen atoms, except the ones from OH functional groups, are omitted for clarity. Selected bond lengths (Å) for **1**: Co–μ_3-Cl 2.4629(6), 2.5046(7), 2.5896(7); Co–Cl 2.3558(7); Co–N 2.105(2); Co–O 2.090(2). Selected bond lengths (Å) for **2**: Ni–μ_3-Cl 2.4264(9), 2.4700(9), 2.5042(9); Ni–Cl 2.347(1); Ni–N 2.052(3); Ni–O 2.072(3). Colour code: H, off-white; C, dark-grey; N, dark-blue; O, red; S; yellow; Cl, light-green; M, light-blue. ORTEPs of the structures are reported in the Supporting Information with complete labeling scheme of the heteroatoms (Figures S1 and S2).

Magnetism and magnetochemical modelling

The molecular magnetism of complexes **1** and **2** as discrete objects was studied by the dc and ac magnetic susceptibility measurements and the results obtained were analysed using the CONDON 2.0 computational framework.[10] The magnetochemical analysis of Co(II) complexes is frequently complicated by a multitude of factors, notably the fact that the Co(II) free-ion ^4F ground term is separated from the first excited term ^4P by more than 10^4 cm^{-1}.[20] In a weak ligand field with octahedral symmetry, the ^4F term splits into the $^4T_1(F)$, $^4T_2$, and $^4A_2$ states, whereas the ^4P term transforms into a $^4T_1(P)$ state. The magnetic properties of high-spin octahedral Co(II) ($3d^7$) complexes are characterised by a significant temperature dependence of μ_{eff} caused by orbital momentum contributions due to the $^4T_1(F)$ ground state. On the other hand, high-spin octahedral Ni(II) ($3d^8$) complexes with an orbital singlet ground state $^3A_2(F)$ represent near-ideal pure spin systems.[21]

Due to the two types of ligands (Cl vs. N, O from HL·S) present in **1** and **2**, a proper description of the ligand field around the magnetic centres ought to adopt C_{2v} instead of

precise octahedral symmetry. This, combined with spin-orbit coupling, leads to further splitting of the states into Kramer's doublets (**1**) or B_1 singlets (**2**).

Study of $[Co(\mu_3\text{-}Cl)Cl(\mathbf{HL{\cdot}S})]_4$ (**1**). The temperature dependence of the effective magnetic moment μ_{eff} and of the reciprocal molar susceptibility χ_m^{-1} (dc measurements) for various applied magnetic fields is shown in Figure 4. The μ_{eff} of **1** at 300 K is 9.71 and lies within the range 8.6 – 10.4 expected as a result of spin and first-order orbital contributions for high-spin Co(II) complexes with negligible exchange interaction contributions.[22] Since μ_{eff} shows almost pure single-ion effects and no maximum at low temperatures, no or very weak antiferromagnetic net exchange interactions are anticipated.

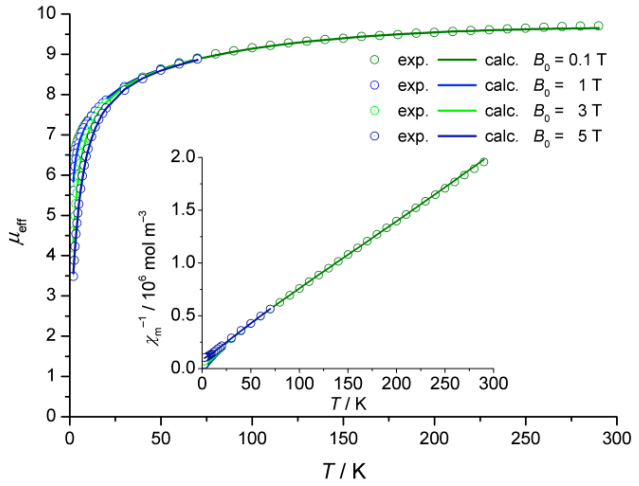

Fig. 4. Temperature dependence of μ_{eff} and χ_m^{-1} (inset) for **1**.

For simulations of the dc susceptibility data, we used our computer program CONDON 2.0[10] which allows to reproduce both intramolecular exchange coupling and single-ions effects: interelectronic repulsion ($\hat{H}_{ee}$), spin–orbit coupling ($\hat{H}_{so}$), ligand-field effect ($\hat{H}_{lf}$), and the Zeeman effect of an applied field ($\hat{H}_{mag}$). In particular, the g value of the electron is a constant of value 2 for all elements. Intramolecular exchange between magnetic centres was modeled using the Heisenberg approach:

$$\hat{H}_{ex} = -J_1(\hat{S}_1{\cdot}\hat{S}_2 + \hat{S}_3{\cdot}\hat{S}_4) - J_2(\hat{S}_1{\cdot}\hat{S}_3 + \hat{S}_2{\cdot}\hat{S}_4 + \hat{S}_1{\cdot}\hat{S}_4 + \hat{S}_2{\cdot}\hat{S}_3).$$

The following standard Racah and spin-orbit constants were employed for Co(II):[20c] B = 1115 cm^{-1}, C = 4366 cm^{-1}, and ζ = 533 cm^{-1}. The ligand-field effects, spin-orbit coupling and exchange coupling have all been taken into account. To limit the number of free parameters, we restricted the modelling procedure to a uniform ligand field environment for all four Co(II) sites. Due to the otherwise enormous demand of main memory, the basis sets for each Co(II) (full basis: 120 microstates per ion, i.e. 120^4 microstates for the whole complex) had to be reduced. An elegant solution is the implementation of the combined model[23] that applies the full Hamiltonian to the ground state (and optionally following excited states) and models the exchange interactions of a definite number of higher excited states in the molecular-field approximation. Thus, this approach includes possible anisotropic exchange interactions and simultaneously reduces the number of fit parameters. Based on an analysis of the splitting of the energy states in a C_{2v}-symmetric ligand-field, it is sufficient to take four microstates (related to $^4B_1$) for the full Hamiltonian and additional 12 (= 8 + 4) for the molecular-field approximation, i.e. 16 microstates for each Co(II) in **1**.

The fit procedure yielded the ligand-field parameters given in Table 1 (Wybourne notation) and a uniform interaction parameter $J_1 = J_2 = -0.14$ cm^{-1}. This best fit describes the structure of **1** with very weakly interacting Co(II) centres, i.e. quasi-isolated centres. The energy gap between the ground and the first excited doublet of a single Co(II) is 45 cm^{-1}, leading to a corresponding gap of 0.04 cm^{-1} for the cubane-like structure.

Table 1. Ligand-field parameters (Wybourne notation) and exchange interaction coupling of **1** (M = Co) and **2** (M = Ni).

	1	**2**
B^2_0 / cm^{-1}	–13800	–8650
B^2_2 / cm^{-1}	32200	22080
B^4_0 / cm^{-1}	–17780	7850
B^4_2 / cm^{-1}	13700	–16920
B^4_4 / cm^{-1}	16600	15700
$J_1 = J_2$ / cm^{-1}	–0.14	+10.6
SQX[a] / %	1.4	1.0

[a] $SQX = (FQ/n)^{1/2}$, $FQ = \Sigma_i\,(\chi_{m,\,obs}(i) - \chi_{m,\,calc}(i))^2/(\chi_{m,\,obs}(i))^2$

The ac susceptibility measurements revealed no significant out-of-phase components for compound **1**, thus confirming the dc measurement observations and indicating no SMM behaviour for this compound. It is also interesting to note that the cubane-type complexes featuring a $\{Co_4(\mu_3\text{-}O_4)\}$ core are usually SMMs.[15,17]

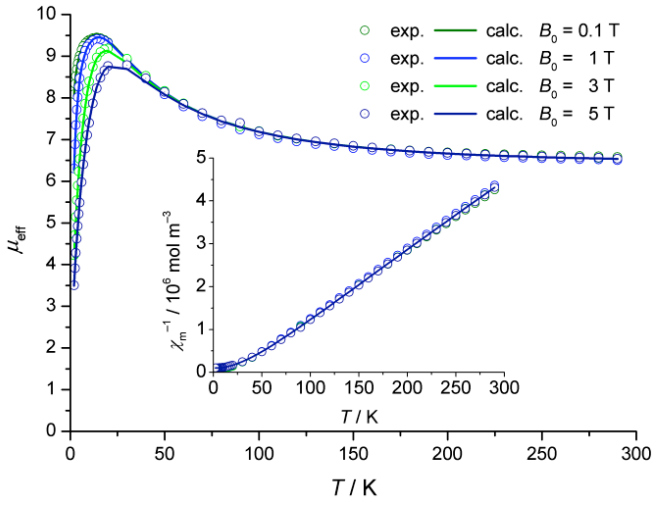

Fig. 5. Temperature dependence of μ_{eff} and χ_m^{-1} (inset) for **2**.

Study of [Ni(μ_3-Cl)Cl(**HL·S**)]$_4$ (**2**). The temperature dependence of the effective magnetic moment μ_{eff} and of the reciprocal molar susceptibility χ_m^{-1} (dc measurements) for various applied magnetic fields is shown in Figure 5. The μ_{eff} of **2** at 300 K is 6.58 and it lies close to the upper limit of the range 5.6 – 7.0 expected for spin contributions for four non-interacting high-spin Ni(II) centres.[22] Since μ_{eff} shows a clear deviation from pure single-ion effects in terms of a maximum at low temperatures, ferromagnetic net exchange interactions are anticipated.

The fitting procedure used for **2** was the same as for **1** modified as follows: the standard Racah and spin-orbit constants for Ni(II)[20c] are: B = 1084 cm^{-1}, C = 4831 cm^{-1}, and ζ = 649 cm^{-1}. The full basis set for Ni(II) of 45 microstates per ion was reduced based on the analysis of the splitting of the energy states. It is sufficient to take three microstates (related to $^3B_1$) for the full Hamiltonian and additional 9 (= 6 + 3) for the molecular-field approximation, i.e. 12 microstates for each Ni(II) in **2**.

The fit yielded the ligand-field parameters given in Table 1 (Wybourne notation) and a uniform interaction parameter J_1 = J_2 = +10.6 cm^{-1}. This best fit describes the structure of **2** with the Ni(II) centres exhibiting ferromagnetic exchange interactions. The energy gap between the ground and the first excited singlet of a single Ni(II) is 14 cm^{-1}, leading to a corresponding gap of 2.3 cm^{-1} for the cubane-like structure.

The ac susceptibility measurements of **2** were performed to determine whether an effective slowing-down of the relaxation of the magnetisation upon an external field change can be observed. This behaviour is a fundamental feature of a SMM.[24,25]

The variation of the in-phase and out-of-phase ac molar susceptibilities (χ_m' and χ_m", respectively) as a function of temperature is depicted in Figure 6. The susceptibility components were measured with an ac amplitude of 3 Gauss and no dc bias, and reveal slow relaxation behaviour up to 3.8 K.

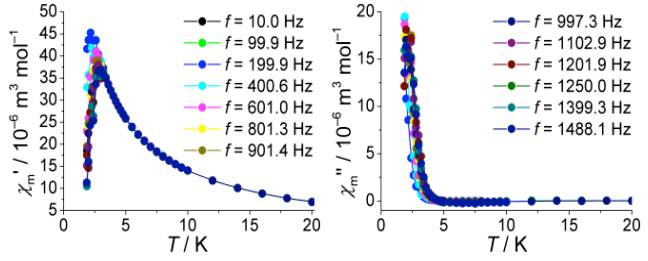

Fig. 6. In-phase (left) and out-of-phase (right) ac susceptibility for **2**.

For each temperature, the data were fitted to a Cole-Cole equation.[26] To determine the relaxation constant τ_0 and effective relaxation energy barrier ΔE on the basis of an Arrhenius expression $\tau = \tau_0 \exp(\Delta E/(k_B T))$, the corresponding parameters of the Cole-Cole fitting procedure above the quantum regime (T > 3 K) was considered (Figure 7).

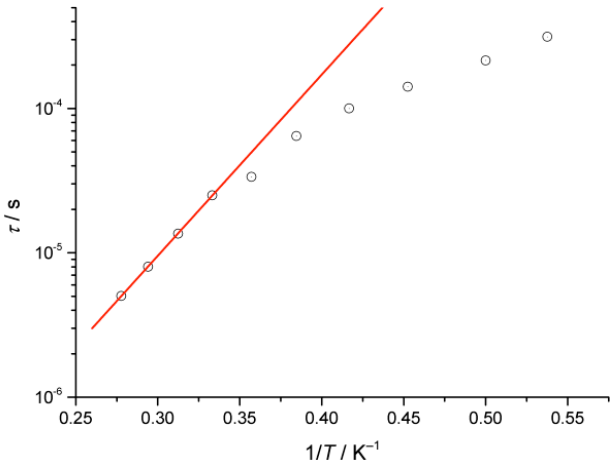

Fig. 7. Arrhenius plot to determine the relaxation constant τ_0 and the effective relaxation energy barrier ΔE of **2**.

The resulting parameters are ΔE = (20.1 ± 0.1) cm^{-1} and τ_0 = (1.64 ± 0.06)·10^{-9} s. In the generalised Debye model, the parameter α quantifies the distribution width τ. The value of α = 0.060 ± 0.041 averaged over all isotherms shows that several relaxation mechanisms seem to exist. Despite the results of the ac susceptibility analysis, no hysteresis of the dc magnetisation is observed down to 1.9 K.

Density functional theory calculations

We conducted DFT calculations on complexes **1** and **2**. The optimised structures, abbreviated respectively **1**$_{DFT}$ and **2**$_{DFT}$, were obtained under the constraints of the C_2 point group at the UBP86-D3[27] level in the high-spin states[28] (see Computational Details). The structural deficiencies issued from the BP86 level of theory are improved with the inclusion of dispersion corrections of D3 generation, especially for the π–π stacking interactions. The optimised structures are, thus, in good agreement with the experimental ones (Table 2).

Table 2. Comparison between the structural parameters of **1**$_{DFT}$ and **2**$_{DFT}$ optimised at the UBP86-D3 level and **1** and **2** determined by single-crystal X-ray crystallography. Bond distances are given in Å and bond angles in deg.

	M = Co		M = Ni	
	1$_{DFT}$	**1**	**2**$_{DFT}$	**2**
M···M	3.638 – 3.769	3.6804(5) – 3.8559(5)	3.577 – 3.644	3.6029(6) – 3.7378(6)
M–μ_3-Cl	2.462 – 2.550	2.4629(6) – 2.5896(7)	2.436 – 2.458	2.4264(9) – 2.5042(9)
M–Cl	2.347	2.3558(7)	2.365	2.347(1)
M–N	2.080	2.105(2)	2.027	2.052(3)
M–O	2.068	2.090(2)	2.058	2.072(3)
O···Cl	3.107	3.233(2) Å	3.086	3.206(3) Å
$\pi_{Py}\cdots\pi_{Py}$	3.921[a]	3.770(2)	3.870[a]	3.757(2)
M–Cl–M	92.4 – 97.5	93.48(2) – 98.38(2)°	93.4 – 96.3	93.88(3) – 97.43(3)°

[a] $d\pi_{Py}\cdots\pi_{Py}$ = 4.725 Å and 4.735 Å for **1**$_{DFT}$ and $d\pi_{Py}\cdots\pi_{Py}$ = 4.568 Å and 4.572 Å for **2**$_{DFT}$ at the non-dispersion corrected UBP86 level.

We estimated the relative energies of tetramerisation (ΔE_{tetra}) of discrete [MCl$_2$(**HL·S**)] units (**1**'$_{DFT}$: M = Co; **2**'$_{DFT}$: M = Ni) involved in the formation of the high-spin cubanes,

[M(μ_3-Cl)Cl(**HL·S**)]$_4$. The tetrahedral and square-planar coordination geometries were postulated for the metal ions in the minimum energy structures of **1**'$_{DFT}$ and **2**'$_{DFT}$, respectively. Indeed, the ground states of the [MCl$_2$(**HL·S**)] complexes differ between **1**'$_{DFT}$ with the S' = 3/2 and **2**'$_{DFT}$ with the S' = 0. As seen in Figure 8, **2**$_{DFT}$ has enhanced thermodynamic stability (by *ca.* 100 kJ·mol^{-1}) in solution when compared to **1**$_{DFT}$ at the DFT level used. In fact, this is compatible with the higher thermal stability of **2** than **1**, according to TGA.

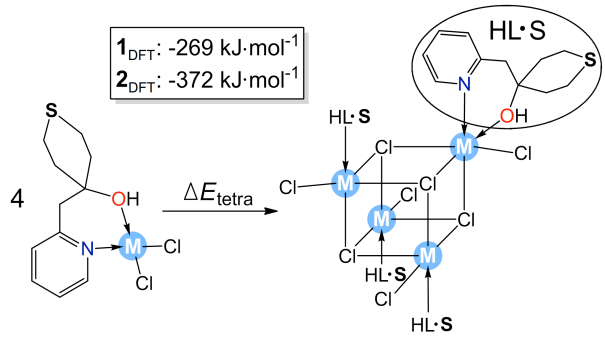

Fig. 8. Relative energies of tetramerisation (ΔE_{tetra}) of discrete [MCl$_2$(**HL·S**)] complexes (**1**'$_{DFT}$: M = Co; **2**'$_{DFT}$: M = Ni) in solution toward the formation of the cubane-like [M(μ_3-Cl)Cl(**HL·S**)]$_4$ structures (**1**$_{DFT}$: M = Co; **2**$_{DFT}$: M = Ni).

We carried out DFT calculations on structures **1** and **2** to help rationalising the experimental information on molecular magnetism. Since the DFT deals with single Slater determinants to describe open-shell electronic configurations instead of spin-adapted states, we applied the *broken-symmetry* approach to compute the energies of the open-shell configurations, namely those with $M_S \leq S_{HS}$. The Ising spin Hamiltonian was applied to get an adequate mapping between the DFT energies and the different spin-polarised states. The M-Cl-M angles in both compounds are close to 95º, a critical value that often separates the FM and AFM regimes. Therefore, it is difficult to anticipate whether the J parameters are positive (FM) or negative (AFM), being close to zero due to the competition between both regimes. By inspection of the structural parameters listed in Table 1, we considered a two-J model based on the presence of two longer (J_1) and four shorter (J_2) M···M distances to determine the sign and magnitude of the magnetic interactions between the local spin moments of M(II) ions. As it is deduced from the μ_{eff} values at high T shown in Figs. 4 and 5 for compounds **1** and **2**, the local spin of Co^{2+} and Ni^{2+} atoms is S = 3/2 and S = 1, respectively. Thus, to extract the J_1 and J_2 parameters we computed the three situations depicted in Fig. 9: the high-spin (S_{HS} = ↑↑↑↑), the intermediate-spin (S_{IS} = ↑↑↑↓) and the low-spin (S_{LS} = ↑↑↓↓) configurations, where each arrow represents S =3/2 for Co, and S = 1 for Ni.

The spin Hamiltonian used to characterise the magnetic coupling parameters contains a summation extending over all the possible interacting spin pairs:

$$\hat{H} = -J_1 \sum_{i,j} \hat{S}_{z,i}\hat{S}_{z,j} - J_2 \sum_{k,l} \hat{S}_{z,k}\hat{S}_{z,l}$$

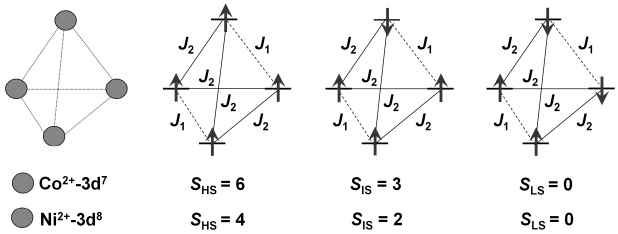

Fig. 9. Three possible orientations of local spin moments (arrows: S = 3/2 for Co, S = 1 for Ni) and total (S, sum of arrows) spin quantum numbers for the cubane-type [M(μ_3-Cl)Cl(**HL·S**)]$_4$ complexes. The coupling constants J_1 and J_2 represent the strength of the interactions between the M ions bridged by μ_3-Cl ligands.

From this model, the energy spectrum for M = Ni^{2+} is:

$$E_{HS} = -2J_1 - 4J_2\,;\quad E_{IS} = 0\,;\quad E_{LS} = -2J_1 + 4J_2$$

and for M = Co^{2+} is:

$$E_{HS} = -\tfrac{9}{2}J_1 - 9J_2\,;\quad E_{IS} = 0\,;\quad E_{LS} = -\tfrac{9}{2}J_1 + 9J_2$$

The main results arising from computations performed with the B3LYP-D3 and PBE0 density functionals for the optimised (**1**$_{DFT}$ and **2**$_{DFT}$) and experimental (**1** and **2**) geometries are listed in Table 3. The agreement between the PBE0 and B3LYP values of J_1 and J_2 is significant and gives robustness to the conclusions derived from computations. An estimate for the molecular zero-field splitting (ZFS) parameter, D, was computed applying the *giant spin approximation*. This model considers that a single total molecular spin (S) prevails by the strong alignment of the local spin moments. For the total spin, the anisotropy can be calculated with $H^{GSA} = S\mathbf{D}S$. The applicability of this model is subject to the fact that the strength of the isotropic coupling of spin moments be much larger that that of the anisotropic coupling, $J >> D$. This is the so-called 'strong exchange limit'. On the other side, $D \sim J$ characterises the 'weak exchange limit' and the giant spin approximation cannot be properly applied. We will see later that compound **1** is in the weak exchange limit and the extraction of a total D is an inaccurate procedure. The local ZFS parameters for Co^{2+} and Ni^{2+} are also computed and discussed in this section. The following discussion is based on the PBE0 results obtained with experimental structures only.

Table 3. Magnetic quantities[a] of [M(μ_3-Cl)Cl(**HL·S**)]$_4$ complexes computed at the UB3LYP-D3 and UPBE0 levels.[b]

	UB3LYP-D3				UPBE0			
	M = Co		M = Ni		M = Co		M = Ni	
	1$_{DFT}$	**1**	**2**$_{DFT}$	**2**	**1**$_{DFT}$	**1**	**2**$_{DFT}$	**2**
J_1	–1.34	–8.07	19.56	18.15	–0.54	–1.25	16.74	15.93
J_2	3.99	5.91	17.44	13.91	3.50	2.96	15.43	12.40
D[c]						0.81		–0.44

[a] Values in cm^{-1}. [b] For each compound, we used the UBP86-D3 optimised structure or the X-ray one. [c] ZFS molecular parameters calculated assuming the giant spin approximation.

For structure **1**, present DFT calculations and application of the Ising hamiltonian give a negative J_1 = –1.25 cm^{-1} and a positive J_2 = 2.96 cm^{-1}, leading to an parallel spin alignment (S_{HS} = 6 situation, see Fig. 9). This result is in apparent contradiction with the

experimental evidence (Fig. 4), namely a low-spin ground state. However, magnetic anisotropy may bridge both results. The calculation of the total molecular D = 0.81 cm^{-1} may explain the low-spin ground state since it stabilizes the M_S = 0 state by virtue of $E = D{\cdot}M_S^2$ (considering a small rhombic anisotropy, $E << D$), the Kramer's doublets M_S = ±1, ±2, …, ±6 appearing above the M_S = 0 state. Even though, the splittings of the various M_S states computed with this D parameter span an energy range (29.2 cm^{-1}) that merges with the energy separation of the S = 6 and S = 3 states (computed 21 cm^{-1}). In other words, we are in the 'weak exchange limit' and the giant spin model is inappropriate. To somehow have an estimate of the local D parameter in Co^{2+},[29] we studied the single-ion (local) ZFS using a $CoZn_3$ model where the Co^{2+} centre is in its *real* molecular environment, obtaining D = 4.0 cm^{-1}. This value, compared to J_1 = –1.25 cm^{-1} and J_2 = 2.96 cm^{-1}, confirms the 'weak exchange limit' scenario in **1**. In principle, a more elaborate description of the iso- and anisotropic coupling is mandatory, although for such a tetranuclear compound the quantum mechanical extraction of accurate parameters is nearly unaffordable. Despite that, even the crude DFT calculation presented here could qualitatively explain the absence of a net spin moment in the ground state of [Co(μ_3-Cl)Cl(**HL·S**)]$_4$.

For the nickel compound, the computed J_1 and J_2 isotropic coupling constants are positive and similar (Table 3). They are also larger than in **1**, resulting in ferromagnetically coupled local spins and a molecular high-spin ground state, S = 4. The energy difference between the lowest S = 4 and the first excited S = 2 states is ΔE = 81 cm^{-1} from calculations. This is a sufficiently large value to assume the 'strong exchange limit', that is, the isotropic exchange is much stronger than the ZFS and the giant spin approximation can be applied. The axial anisotropy parameter (D) computed with the PBE0 functional is therefore relevant thanks to the strong ferromagnetism of the system. For **2**, D = –0.44 cm^{-1} with a negligible rhombic anisotropy (E/D = 0.0002 cm^{-1}). The main implication is that **2** has an easy axis of magnetisation with a $M_s \neq 0$ ground state. The same conclusion concerning the ground state can be extracted from the curve in Fig. 5. The computed molecular D parameter produces a ZFS of the M_S = ±4, ±3, …, 0 states with respectively $E = D{\cdot}M_S^2$ = –5.6, –2.5, –0.3, +1.0 and +1.5 cm^{-1} with respect to the S = 4 manifold. In this regard, the compound has the ingredients to behave as a SMM. The single-ion (local) magnetic anisotropy obtained with a $NiZn_3$ model gives D = –0.79 cm^{-1} using its experimental structure. This is in agreement with a total $M_s \neq 0$ ground state due to the dominant FM coupling deduced from J_1 and J_2. If the local $M_s \neq 0$ are ferromagnetically aligned we recover the same solution obtained through the giant spin approximation to get the lowest total M_S.

Figure 10 shows the computed (DFT/PBE0) low energy spectrum for complex **2**. The cubane-type Ni(II) complex thus reveals as a candidate to join the family of SMMs and this result is consistent with the magnetochemical data of the compound. To better understand a physical picture of the ground states and magnetic interactions within **2**, we plan to perform mK magnetisation measurements of this compound at high magnetic fields in the near future.

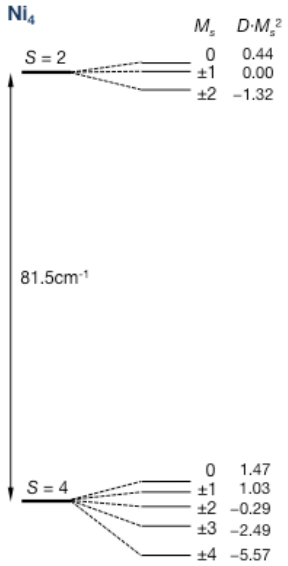

Fig. 10. Low energy spectra for compound **1**, showing the energy splittings of the lowest S levels and the associated M_s states (in cm^{-1}) obtained from the J and D values in Table 3. To estimate the ZFS of the S = 2 manifold we applied the same D parameter as for S = 4 as an approximation. The separation between consecutive S levels, caused by the isotropic coupling (J parameters) is large compared to the ZFS parameter, allowing us to apply the strong exchange limit. It can be deduced that complex **2** has low-lying $M_s \neq 0$ states.

Conclusions

We demonstrated that two new *iso*structural complexes [M(μ_3-Cl)Cl(**HL·S**)]$_4$ (**1**: M = Co and **2**: M = Ni) may have very different spin behaviour caused by factors such as the nature of the transition metal ions, ligand-field effects, and magnetic anisotropy characteristics. In this regard, DFT calculations permitted a detailed modelling of the distinct coupling pathways (J_1 and J_2). In compound **1**, there is one positive and one negative coupling constants that sum up to a high-spin S = 6 ground state. This might not be in contradiction with experiments if the positive ZFS parameter, D, is positive as the DFT calculations on a single Co^{2+} ion suggest. In this scenario, a M_S = 0 ground state is predicted. It must be pointed out that the accurate description of the magnetic properties of **1** is far beyond the range of the DFT. In complex **2** the two J constants are positive leading to a S = 4 ground state. The total D < 0 magnetic anisotropy in complex **2** suggests an easy axis of magnetization ($M_s \neq 0$ ground state), in agreement with the FM behavior observed. This complex is thus envisaged as a SMM. In view of the structure of the Ni(II) complex **2** with structurally exposed S functional groups as part of the pyridyl-alcohol ligands (**HL·S**), studies of this SMM on metal surfaces represent an important step in the development of tailored-made transition-metal complexes with magnetic functions for single-

molecule electronics and nanotechnology. The availability of the new **HL·S** ligand may help the development of an intriguing class of compounds based on exchange-coupled transition metal, lanthanide, and actinide ions with high relevance to studies of electron transport through single-molecule junctions.[30] Furthermore, the *iso*structural compounds **1** and **2** generate considerable interest for ultrafast time-resolved spectroscopy and photophysics since it is of high importance to gain a better understanding of the influence of intramolecular exchange between magnetic centres on the absorption and emission processes in coordination complexes.[31] Finally, the explanatory concepts for physics and magnetostructural correlations in transition metal complexes containing $\{M_4(\mu_3\text{-}N_3)_4\}$, $\{M_4(\mu_3\text{-}O_4)\}$ and $\{M_4(\mu_3\text{-}X_4)\}$ (X = F, Cl) cubane cores[32] with a high sensitivity to the ligands and their coordination schemes are to be established. All these aspects are currently explored in our laboratories by experimental and computational methods.

Experimental and Computational

Materials and methods

$[NiCl_2(dme)]$ was prepared following a published procedure.[33] The reactions were performed under dry argon using standard Schlenk techniques. All solvents used were freshly distilled before use. NMR spectra were recorded at room temperature on a Bruker AVANCE 300 spectrometer (^{1}H, 300 MHz; ^{13}C, 75.47 MHz) and referenced using the residual proton solvent (^{1}H) or solvent (^{13}C) resonance. Chemical shifts (δ) are given in ppm. The FTIR spectra were collected on a ThermoNicolet 6700 spectrometer equipped with a diamond crystal SMART ORBIT ATR accessory. The FTIR spectra of single crystals were collected by a Thermo-Nicolet Centaurus FTIR microspectrometer in diamond window microcompression cells. Unless otherwise stated, all products were commercial and used as received.

Synthesis of 4-(pyridin-2-ylmethyl)tetrahydro-2H-thiopyran-4-ol (HL·S)

A solution of *n*-BuLi (16.2 mL, 26.00 mmol, 1.60 M in hexane) was added dropwise over 15 min to a solution of 2-picoline (2.420 g, 26.00 mmol) in 150 mL of THF at –78 °C. After complete deprotonation, a red solid precipitated and after further stirring for 1 h at –78 °C a solution of tetrahydro-4H-thiopyran-4-one (3.00 g, 26.00 mmol) in 50 mL of THF was added dropwise to the suspension. The resulting pale yellow solution was allowed to reach room temperature overnight. After addition of 100 mL of a saturated solution of NH_4Cl in water, the reaction mixture was extracted with Et_2O (3 × 30 mL). The organic phases were collected and dried with Na_2SO_4, which was then filtered off. Evaporation of the volatiles produced brown crystals of **HL·S**. Yield: 4.00 g (73%). Anal. Calcd. for $C_{11}H_{15}NOS$ (209.31): C, 63.12; H, 7.22; N, 6.69. Found: C, 62.96; H, 6.87; N, 6.61. FTIR: ν_{max}(solid)/cm^{-1}: 3210s, 3078vw, 3055vw, 3021vw, 2955w, 2917s, 1592s, 1569s, 1480s, 1423vs, 1353vw, 1339w, 1320m, 1302m, 1277s, 1259s, 1242w, 1222mw, 1164vw, 1149w, 1140m, 1101s, 1080m, 1054vs, 1020w, 1002s, 937s, 921vs, 898vw, 882m, 838vw, 819vw, 790m, 772m, 755vs, 721m, 670w, 658m, 637w, 628m, 602w, 479s, 435m, 428m, 406vs, 366vs, 288s, 270vs, 246m, 219s, 161vw, 151vw, 129vs, 119w, 102vs. In the following NMR description, the atom numbering used is shown in Figure 11. ^{1}H NMR ($CDCl_3$, 300 MHz) δ: 8.61 (brd, 1H, $^3J_{H,H}$ = 4.9 Hz, H_8Py), 7.76 (dt, 1H, $^3J_{H,H}$ = 7.6 and 1.8 Hz, H_6Py), 7.32-7.28 (dd, 1H, $^3J_{H,H}$ = 7.5 Hz and 4.9 Hz, H_7Py), 7.25 (d, 1H, $^3J_{H,H}$ = 7.6 Hz, H_5Py), 6.07 (br, 1H, OH), 3.24-3.14 (m, 2H, CH of C_4 and $C_{4'}$), 3.00 (s, 2H, C_1), 2.54-2.47 (m, 2H, CH of C_4 and $C_{4'}$), 2.00-1.93 (m, 2H, CH of C_3 and $C_{3'}$), 1.85-1.76 (m, 2H, CH of C_3 and $C_{3'}$) ppm. $^{13}C\{^1H\}$ NMR ($CDCl_3$, 75.5 MHz) δ: 158.98 (s, C_{ipso}Py), 148.45 (s, C_8Py), 137.18 (s, C_6Py), 124.80 (s, C_5, Py), 121.84 (s, C_7, Py), 69.92 (s, C_2), 48.12 (s, C_1), 38.88 (s, C_4, $C_{4'}$), 24.47 (s, C_3, $C_{3'}$) ppm.

Synthesis of $[Co(\mu_3\text{-}Cl)Cl(HL\cdot S)]_4$ (1)

A slurry of anhydrous $CoCl_2$ (0.252 g, 1.94 mmol) in 30 mL of THF was sonicated for 1 h until complete dissolution. A solution of **HL·S** (0.406 g, 1.94 mmol) in 15 mL of THF was then added and the reaction mixture was stirred for 2 h at room temperature. The volatiles were removed under reduced pressure and the blue powder obtained was dissolved in CH_2Cl_2 and filtered. The filtrate was then layered with Et_2O. Octahedral blue crystals of **1**, suitable for X-ray diffraction analysis, were obtained at room temperature after 3 days. Yield: 0.414 g (63%). Anal. Calcd. for $C_{44}H_{60}Cl_8Co_4N_4O_4S_4\cdot 2CH_2Cl_2$ (1526.47): C, 36.19; H, 4.22; N, 3.67. Found: C, 35.82; H, 4.45; N 3.62. FTIR: ν_{max}(KBr pellet)/cm^{-1}: 3178mbr, 2932mbr, 2855vw, 1605vs, 1570m, 1560w, 1541w, 1533vw, 1508vw, 1483m, 1443s, 1400sh, 1351w, 1294w, 1269m, 1244w, 1213m, 1158w, 1141vw, 1124vw, 1108w, 1077w, 1036vs, 1020s, 993w, 969vw, 920s, 866m, 834w, 774vw, 760m, 731s, 715w, 699w, 669vw, 658vw, 645w, 608vw, 572w, 513w, 481w, 450vw, 425m, 309w, 296w, 285w, 256s, 230sh, 213vs, 200sh, 143w, 135w, 130w, 122w, 115w, 102w.

Synthesis of $[Ni(\mu_3\text{-}Cl)Cl(HL\cdot S)]_4$ (2)

To a slurry of $[NiCl_2(dme)]$ (0.315 g, 1.43 mmol) in 15 mL of THF was added a solution of **HL·S** (0.300 g, 1.43 mmol) in 15 mL of THF. The reaction mixture was stirred for 2 h at room temperature whereupon the orange dispersion became a yellow solution. The volatiles were evaporated under reduced pressure and the yellow powder obtained was dissolved in CH_2Cl_2. The solution was filtered and the filtrate was layered with Et_2O. Octahedral yellow crystals of **2**, suitable for X-ray diffraction analysis, were obtained at room temperature after 3 days. Yield: 0.360 g (74%). Anal. Calcd. for $C_{44}H_{60}Cl_8Ni_4N_4O_4S_4$ (1355.64): C, 38.98; H, 4.46; N, 4.13. Found: C, 39.03; H, 4.67; N 4.04. FTIR: ν_{max}(KBr pellet)/cm^{-1}: 3178brs, 3113brs, 2957w, 2943vw, 2926w, 2914w, 2857w, 2800vw, 1607s, 1571m, 1486m, 1446vs, 1430shw, 1424vw, 1397w, 1362vw, 1343w, 1318vw, 1295vw, 1284vw, 1259s, 1233m, 1219vw, 1210vw, 1203vw, 1159w, 1145w, 1112s, 1091vw, 1078vw, 1065vw, 1053w, 1039s, 1024w, 1013w, 1000vw, 945vw, 918vs, 865w, 854m, 829m, 784sh, 775s, 756s, 737vw, 715ms, 693w, 651ms, 638w, 628vw, 608vw, 576m, 517m, 488m, 470vw, 453w, 429m, 405vw, 352m, 335w, 302vw, 263s, 225vs, 205sh, 182vw, 150w, 131vw, 121vw, 104vw.

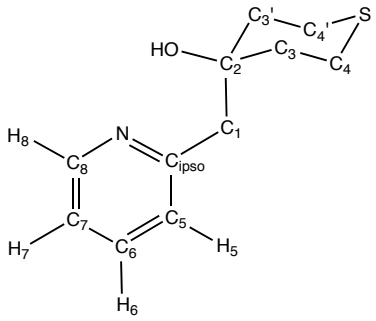

Figure 11. Atom numbering scheme used for the NMR description of ligand **HL·S**.

X-ray crystallography

Suitable crystals for the X-ray analyses of **1** and **2** were obtained as described above. The intensity data were collected on an APEX II DUO Kappa-CCD area detector diffractometer[34] (graphite monochromated Mo-Kα radiation, λ = 0.71073 Å). The structures were solved by direct methods (SHELXS-97) and refined by full-matrix least-squares procedures (based on F^2, SHELXL-97)[35] with anisotropic thermal parameters for all the non-hydrogen atoms. The hydrogen atoms were introduced into the geometrically calculated positions (SHELXL-97 procedures) and refined *riding* on the corresponding parent atoms, except the ones from OH functional groups (see below). A summary of crystal data and structure refinements for **1** and **2** is given in Table S1 of the Supporting Information and in footnote 14. In both structures, a dichloromethane molecule was found disordered over at least six positions with no atom in common. Any attempt to give a reasonable model of this disorder, severely affecting the model quality, failed. A PLATON SQUEEZE procedure[36] was applied using complete anisotropic models, resulting in an improved model quality. Details are given in the CIF files. The OH hydrogen atom was found in the difference maps and was refined with a restrained O–H distance of 0.9 Å. CCDC 964328 for **1** and 964329 for **2** contain the supplementary crystallographic data that can be obtained free of charge from the Cambridge Crystallographic Data Centre via www.ccdc.cam.ac.uk/data_request/cif.

Magnetic susceptibility measurements

Magnetic susceptibility data of **1** and **2** were recorded using a Quantum Design MPMS-5XL SQUID magnetometer for direct current (dc) as well as alternating current (ac) measurements. The polycrystalline samples were compacted and immobilised into cylindrical PTFE capsules. The dc susceptibility data were acquired as a function of the field (0.1−5.0 T) and temperature (2.0−290 K). The ac susceptibility data were measured in the absence of a static bias field in the frequency range 10−1500 Hz (T = 1.8−50 K, B_{ac} = 3 G). Only compound **2** exhibited out-of-phase components above 1.8 K. All data were corrected for the contribution of the sample holder (PTFE capsule) and the diamagnetic contributions of compounds **1** and **2** calculated from tabulated values (-9.59×10^{-9} m^3 mol^{-1} and -8.51×10^{-9} m^3 mol^{-1}, respectively).

Computational details and theory

Density functional theory (DFT) geometry optimisations were performed using the Amsterdam Density Functional (ADF) program.[37,38] The numerical integration was performed using the procedure developed by te Velde *et al*.[38g,h] The molecular orbitals were expanded in a large set of uncontracted Slater-type orbitals (STOs) of triple-ζ quality augmented with two sets of polarisation functions for all atoms (TZ2P basis set[38i]), i.e. 2p and 3d on H, 3d and 4f on C, N, O, S, and Cl, and 4d and 4f on Co and Ni. The core shells of C, N, and O (1s), S and Cl (up to 2p), and Co and Ni (up to 2p) were treated by the frozen (small) core approximation.[38c] An auxiliary set of s, p, d, f, and g STOs was used to fit the molecular density and to represent the Coulomb and exchange potentials accurately in each self-consistent field cycle.[38j] All the structures were optimised with the BP86 density functional as it has been shown to be one of the three best generalised gradient approximation (GGA) DFT functionals (along with PBE and PW91) for geometry optimisations with the ADF program package.[39] The electronic exchange was described by Slater's Xα potential[38l] with self-consistent nonlocal corrections of Becke[38m,n] and the electron correlation was treated in the Vosko-Wilk-Nusair (VWN) parameterisation[38o] with self-consistent nonlocal corrections of Perdew[38p] (BP86).[38q] The Grimme's dispersion correction of D3-generation[27,40] for the DFT functionals was implemented (referred to as BP86-D3[41]). A spin-restricted and spin-unrestricted formalism was applied at the GGA level. Scalar relativistic effects were accounted for using the Zeroth-Order Regular Approximation (ZORA).[42] All DFT calculations were carried out taking into account the homogeneous THF (ε = 7.58) solvent medium used during the synthetic preparation of **1** and **2**. ZORA-(U)BP86-D3/TZ2P was combined with the COnductor-like Screening MOdel (COSMO) of solvation with the solvent-excluding surface (SES) to define the cavities surrounding the complexes.[43] The atomic radii were issued from the ADF program. The minimum energy structures were verified through vibrational analysis with detailed surface scans to have zero imaginary frequencies.[44] The single point energy calculations of the UBP86-D3 equilibrium structures $\mathbf{1}_{DFT}$ (M = Co) and $\mathbf{2}_{DFT}$ (M = Ni) and the X-ray crystal structures of **1** and **2** were also performed at COSMO/ZORA-UPBE0/TZ2P and COSMO/ZORA-UB3LYP-D3/TZ2P to obtain the energy differences between the high-spin and *broken-symmetry* states of the specified compounds. At these levels of theory, the non-dispersion corrected, hybrid UPBE0 functional[45] and dispersion-corrected (D3), hybrid UB3LYP functional[46] were used in conjunction with the all-electron TZ2P basis sets implemented for all elements. The Zero-Field Splitting parameter, D, was computed with the ORCA program[47] with the perturbative Pederson-Khanna method,[48] taking the experimental geometries of **1** and **2** and performing single point calculations at the DFT-UPBE0/TZ2P level of theory.

Acknowledgements

We are grateful to the CNRS, the Ministère de la Recherche (Paris), the DFH/UFA (International Research Training Group 532-GRK532, PhD grant to A.G.), the International Centre for Frontier Research in Chemistry, Strasbourg (icFRC, http://www.icfrc.fr), the DFG (postdoctoral reintegration fellowship to K.Y.M.) and the Spanish Government (Project No. CTQ2011-23140 and the Ramón y Cajal program with

grant No. RYC-2008-02493 to X.L.). We also thank the Service de Radiocristallographie, Institut de Chimie (UMR 7177 CNRS-UdS) for the X-ray diffraction studies.

Notes and references

[a] *Laboratoire de Chimie de Coordination, Institut de Chimie (UMR 7177 CNRS), Université de Strasbourg, 4 rue Blaise Pascal, F-67081 Strasbourg, France; E-mail: braunstein@unistra.fr.*
[b] *Institut für Anorganische Chemie, RWTH Aachen University, Landoltweg 1, 52074 Aachen, Germany; E-Mail: kirill.monakhov@ac.rwth-aachen.de, paul.koegerler@ac.rwth-aachen.de.*
[c] *Departament de Química Física i Inorgànica, Universitat Rovira i Virgili, c/Marcel·lí Domingo s/n, 43007 Tarragona, Spain.*
[d] *Institució Catalana de Recerca i Estudis Avançats (ICREA), Passeig Lluís Companys 23, 08010, Barcelona, Spain.*
[e] *Peter Grünberg Institute (PGI-6), Forschungszentrum Jülich, 52425 Jülich, Germany.*

† Electronic Supplementary Information (ESI) available: [Crystallographic data of **1** and **2** and details of DFT calculations. This material is available free of charge via the Internet at http://pubs.acs.org]. See DOI: 10.1039/b000000x/

1 (a) F. Speiser, L. Saussine and P. Braunstein, *Inorg. Chem.,* 2004, **43**, 4234; (b) A. Kermagoret and P. Braunstein, *Dalton Trans.,* 2008, 1564.
2 (a) J. Zhang, P. Teo, R. Pattacini, A. Kermagoret, R. Welter, G. Rogez, T. S. A. Hor and P. Braunstein, *Angew. Chem. Int. Ed.,* 2010, **49**, 4443; (b) L. Kayser, R. Pattacini, G. Rogez and P. Braunstein, *Chem. Commun.,* 2010, **46**, 6461; (c) S. Hameury, L. Kayser, R. Pattacini, G. Rogez, W. Wernsdorfer and P. Braunstein, *Dalton Trans.,* 2013, **42**, 5013.
3 R. Pattacini, P. Teo, J. Zhang, Y. Lan, A. K. Powell, J. Nehrkorn, O. Waldmann, T. S. A. Hor and P. Braunstein, *Dalton Trans.,* 2011, **40**, 10526.
4 K. Yu. Monakhov, X. López, M. Speldrich, J. van Leusen, P. Kögerler, P. Braunstein and J. M. Poblet, *Chem. Eur. J.,* 2014, DOI: 10.1002/chem.201304177.
5 (a) L. Bogani and W. Wernsdorfer, *Nat. Mater.,* 2008, **7**, 179; (b) M. Mannini, F. Pineider, P. Sainctavit, C. Danieli, E. Otero, C. Sciancalepore, A. Maria Talarico, M.-A. Arrio, A. Cornia, D. Gatteschi and R. Sessoli, *Nat. Mater.,* 2009, **8**, 194; (c) A. Cornia, M. Mannini, P. Sainctavit and R. Sessoli, *Chem. Soc. Rev.,* 2011, **40**, 3076; (d) M. J. Rodriguez-Douton, M. Mannini, L. Armelao, A.-L. Barra, E. Tancini, R. Sessoli and A. Cornia, *Chem. Commun.,* 2011, **47**, 1467.
6 (a) G. Christou, D. Gatteschi, D. N. Hendrickson and R. Sessoli, MRS *Bulletin,* 2000, **25**, 66; (b) A. J. Nelson, J. G. Reynolds and G. Christou, *MRS Symp. Proc.,* 2001, **635**, C4.13.1; (c) W. Wernsdorfer, N. Aliaga-Alcalde, D. N. Hendrickson and G. Christou, *Nature,* 2002, **416**, 406; (d) J. R. Long, *In Chemistry of Nanostructured Materials*; Yang, P., Ed.; World Scientific Publishing: HongKong, 2003, p. 291; (e) G. Christou, *Polyhedron,* 2005, **24**, 2065; (f) C. J. Milios, A. Vinslava, W. Wernsdorfer, S. Moggach, S. Parsons, S. P. Perlepes, G. Christou and E. K. Brechin, *J. Am. Chem. Soc.,* 2007, **129**, 2754; (g) O. Waldmann, *Inorg. Chem.,* 2007, **46**, 10035; (h) R. Bagai and G. Christou, *Chem. Soc. Rev.,* 2009, **38**, 1011.
7 (a) A. Ulman, *Chem. Rev.*, 1996, **96**, 1533; (b) F. Schreiber, *Prog. Surf. Sci.,* 2000, **65**, 151; (c) J. C. Love, L. A. Estroff, J. K. Kriebel, R. G. Nuzzo and G. M. Whitesides, *Chem. Rev.,* 2005, **105**, 1103; (d) I. S. Kristensen, D. J. Mowbray, K. S. Thygesen and K. W. Jacobsen, *J. Phys.: Condens. Matter,* 2008, **20**, 374101; (e) L. Kankate, A. Turchanin and A. Gölzhäuser, *Langmuir,* 2009, **25**, 10435; (f) M. del Carmen Gimenez-Lopez, M. T. Räisänen, T. W. Chamberlain, U. Weber, M. Lebedeva, G. A. Rance, G. A. D. Briggs, D. Pettifor, V. Burlakov, M. Buck and A. N. Khlobystov, *Langmuir,* 2011, **27**, 10977; (g) H. Rath, G. A. Timco, V. Corradini, A. Ghirri, U. del Pennino, A. Fernandez, R. G. Pritchard, C. A. Muryn, M. Affronte and R. E. P. Winpenny, *Chem. Commun.,* 2013, **49**, 3404.
8 (a) M. W. J. Beulen, B. -H. Huisman, P. A. van der Heijden, F. C. J. M. van Veggel, M. G. Simons, E. M. E. F. Biemond, P. J. de Lange and D. N. Reinhoudt, *Langmuir,* 1996, **12**, 6170; (b) C.-J. Zhong, R. C. Brush, J. Anderegg and M. D. Porter, *Langmuir,* 1999, **15**, 518; (c) J. Noh, T. Murase, K. Nakajima, H. Lee and M. Hara, *J. Phys. Chem. B,* 2000, **104**, 7411; (d) H. L. Tierney, J. W. Han, A. D. Jewell, E. V. Iski, A. E. Baber, D. S. Sholl and E. C. H. Sykes, *J. Phys. Chem. C,* 2011, **115**, 897; (e) P. Angelova, E. Solel, G. Parvari, A. Turchanin, M. Botoshansky, A. Gölzhäuser and E. Keinan, *Langmuir*, 2013, **29**, 2217.
9 For pendant thioether functions in transition-metal complexes see, e.g., recent studies: (a) V. Rosa, C. Fliedel, A. Ghisolfi, R. Pattacini, T. Avilés and P. Braunstein, *Dalton Trans.,* 2013, **42**, 12109 and references cited therein; (b) A. Ghisolfi, C. Fliedel, V. Rosa, R. Pattacini, A. Thibon, K. Yu. Monakhov and P. Braunstein, *Chem. Asian J.,* 2013, **8**, 1795.
10 M. Speldrich, H. Schilder, H. Lueken, P. Kögerler, *Isr. J. Chem.*, 2011, **51**, 215.
11 (a) L. Noodleman, *J. Chem. Phys.,* 1981, **74**, 5737; (b) M. Orio, D. A. Pantazis and F. Neese, *Photosynth. Res.,* 2009, **102**, 443; (c) F. Neese, *Coord. Chem. Rev.,* 2009, **253**, 526 and references cited therein.
12 Crystal data for **1**: $C_{44}H_{60}Cl_8Co_4N_4O_4S_4$, M = 1356.52, tetragonal, a = 19.2769(8) Å, b = 19.2769(8) Å, c = 18.5886(8) Å, α = 90.00°, β = 90.00°, γ = 90.00°, V = 6907.5(5) Å^3, T = 173(2) K, space group $I4_1/a$, Z = 4, μ = 1.410 mm^{-1}, 14447 reflections measured, 5026 independent reflections (R_{int} = 0.0268). The final R_1 values were 0.0451 ($I > 2\sigma(I)$). The final $wR(F^2)$ values were 0.1184 ($I > 2\sigma(I)$). The final R_1 values were 0.0613 (all data). The final $wR(F^2)$ values were 0.1284 (all data). The goodness of fit on F^2 was 1.083. Crystal data for **2**: $C_{44}H_{60}Cl_8Ni_4N_4O_4S_4$, M = 1355.64, tetragonal, a = 19.091(1) Å, b = 19.091(1) Å, c = 18.729(1) Å, α = 90.00°, β = 90.00°, γ = 90.00°, V = 6826.5(8) Å^3, T = 173(2) K, space group $I4_1/a$, Z = 4, μ = 1.558 mm^{-1}, 39794 reflections measured, 3351 independent reflections (R_{int} = 0.0261). The final R_1 values were 0.0546 ($I > 2\sigma(I)$). The final $wR(F^2)$ values were 0.1257 ($I > 2\sigma(I)$). The final R_1 values were 0.0623 (all data). The final $wR(F^2)$ values were 0.1314 (all data). The goodness of fit on F^2 was 1.167.
13 R. D. Shannon, *Acta Cryst.,* 1976, **A32**, 751.
14 B. Cordero, V. Gómez, A. E. Platero-Prats, M. Revés, J. Echeverría, E. Cremades, F. Barragán and S. Alvarez, *Dalton Trans.,* 2008, 2832.
15 For Co_4 cubane-type complexes, see: (a) K. Dimitrou, K. Folting, W. E. Streib and G. Christou, *J. Am. Chem. Soc.,* 1993, **115**, 6432; (b) K. Dimitrou, K. Folting, W. E. Streib and G. Christou, *J. Chem. Soc., Chem. Commun.,* 1994, 1385; (c) A. Tsohos, S. Dionyssopoulou, C. P. Raptopoulou, A. Terzis, E. G. Bakalbassis and S. P. Perlepes, *Angew. Chem. Int. Ed.,* 1999, **38**, 983; (d) T. A. Hudson, K. J. Berry, B. Moubaraki, K. S. Murray and R. Robson, *Inorg. Chem.,* 2006, **45**, 3549; (e) M.-H. Zeng, M.-X. Yao, H. Liang, W.-X. Zhang and X.-M. Chen, *Angew. Chem. Int. Ed.,* 2007, **46**, 1832; (f) K. W. Galloway, A. M. Whyte, W. Wernsdorfer, J. Sanchez-Benitez, K. V. Kamenev, A. Parkin, R. D. Peacock and M. Murrie, *Inorg. Chem.,* 2008, **47**, 7438; (g) B. Moubaraki, K. S. Murray, T. A. Hudson and R. Robson, *Eur. J. Inorg. Chem.,* 2008, 4525; (h) J. Liu, S. Datta, E. Bolin, J. Lawrence, C. C. Beedle, E.-C. Yang, P. Goy, D. N. Hendrickson and S. Hill, *Polyhedron,* 2009, **28**, 1922; (i) A. Scheurer, A. M. Ako, R. W. Saalfrank, F. W. Heinemann, F. Hampel, K. Petukhov, K. Gieb, M. Stocker and P. Müller, *Chem. Eur. J.,* 2010, **16**, 4784; (j) K. W. Galloway, M. Schmidtman, J. Sanchez-Benitez, K. V. Kamenev, W. Wernsdorfer, M. Murrie, *Dalton Trans.*, 2010, **39**, 4727; (k) L. R. Falvello, E. Forcén-Vázquez, I. Mayoral, M. Tomás and F. Palacio, *Acta Cryst.,* 2011, **C67**, m359; (l) K. Zhang, J. Dai, Y.-H. Wang, M.-H. Zeng and M. Kurmoo, *Dalton Trans.,* 2013, **42**, 5439.
16 For Ni_4 cubane-type complexes, see: (a) M. A. Halcrow, J. C. Huffman and G. Christou, *Angew. Chem., Int. Ed. Engl.,* 1995, **34**,

889; (b) M. A. Halcrow, J.-S. Sun, J. C. Huffman and G. Christou, *Inorg. Chem.,* 1995, **34**, 4167; (c) A. Escuer, M. Font-Bardía, S. B. Kumar, X. Solans and R. Vicente, *Polyhedron,* 1999, **18**, 909; (d) J. M. Clemente-Juan, B. Chansou, B. Donnadieu and J.-P. Tuchagues, *Inorg. Chem.,* 2000, **39**, 5515; (e) S. Mukherjee, T. Weyhermüller, E. Bothe, K. Wieghardt and P. Chaudhuri, *Eur. J. Inorg. Chem.,* 2003, 863; (f) M. Moragues-Cánovas, M. Helliwell, L. Ricard, É. Rivière, W. Wernsdorfer, E. Brechin and T. Mallah, *Eur. J. Inorg. Chem.,* 2004, 2219; (g) T. Shiga and H. Oshio, *Sci. Technol. Adv. Mater.,* 2005, **6**, 565; (h) M. Schröter, E. Lork and R. Mews, *Z. Anorg. Allg. Chem.,* 2005, **631**, 1609; (i) G. S. Papaefstathiou, A. Escuer, F. A. Mautner, C. Raptopoulou, A. Terzis, S. P. Perlepes and R. Vicente, *Eur. J. Inorg. Chem.,* 2005, 879; (j) A. Ferguson, J. Lawrence, A. Parkin, J. Sanchez-Benitez, K. V. Kamenev, E. K. Brechin, W. Wernsdorfer, S. Hill and M. Murrie, *Dalton Trans.,* 2008, 6409; (k) Q. Liang, R. Huang, X. Chen, Z. Li, X. Zhang and B. Sun, *Inorg. Chem. Commun.,* 2010, **13**, 1134. (l) J.-P. Sun, L.-C. Li and X.-J. Zheng, *Inorg. Chem. Commun*., 2011, **14**, 877; (m) C. G. Efthymiou, C. Papatriantafyllopoulou, G. Aromi, S. J. Teat, G. Christou and S. P. Perlepes, *Polyhedron,* 2011, **30**, 3022; (n) S.-H. Zhang, N. Li, C.-M. Ge, C. Feng and L.-F. Ma, *Dalton Trans*., 2011, **40**, 3000; (o) S. Petit, P. Neugebauer, G. Pilet, G. Chastanet, A.-L. Barra, A. B. Antunes, W. Wernsdorfer and D. Luneau, *Inorg. Chem.,* 2012, **51**, 6645; (p) S.-Y. Zhang, W.-Q. Chen, B. Hu, Y.-M. Chen, W. Li and Y. Li, *Inorg. Chem. Commun.,* 2012, **16**, 74; (q) A. Scheurer, K. Gieb, M. S. Alam, F. W. Heinemann, R. W. Saalfrank, W. Kroener, K. Petukhov, M. Stocker and P. Muller, *Dalton Trans.,* 2012, **41**, 3553; (r) S. Liu, S. Wang, F. Cao, H. Fu, D. Li and J. Dou, *RSC Adv.,* 2012, ***2***, 1310; (s) J.-P. Costes, G. Novitchi, L. Vendier, G. Pilet, and D. Luneau, *C. R. Chimie,* 2012, **15**, 849; (t) A. N. Ponomaryov, N. Kim, J. Hwang, H. Nojiri, J. van Tol, A. Ozarowski, J. Park, Z. Jang, B. Suh, S. Yoon and K.-Y. Choi, *Chem. Asian J.,* 2013, **8**, 1152; (u) S. T. Meally, S. M. Taylor, E. K. Brechin, S. Piligkos, L. F. Jones, *Dalton Trans.,* 2013, **42**, 10315; (v) S. Shit, M. Nandy, G. Rosair, C. J. Gómez-García, J. J. Borras Almenar and S. Mitra, *Polyhedron,* 2013, **61**, 73; (w) C. Ding, C. Gao, S. Ng, B. Wang and Y. Xie, *Chem. Eur. J.,* 2013, **19**, 9961; (x) J. Liu and S. Hill, *Polyhedron,* 2013, **66**, 147; (y) M. K. Ainooson, I. A. Guzei, L. C. Spencer and J. Darkwa, *Polyhedron*, 2013, **53**, 295.

17 (a) E.-C. Yang, D. N. Hendrickson, W. Wernsdorfer, M. Nakano, L. N. Zakharov, R. D. Sommer, A. L. Rheingold, M. Ledezma-Gairaud and G. Christou, *J. Appl. Phys.,* 2002, **91**, 7382; (b) T. Baruah and M. R. Pederson, *Chem. Phys. Lett.,* 2002, **360**, 144; (c) T. Baruah and M. R. Pederson, *Int. J. Quantum Chem.*, 2003, **93**, 324.

18 (a) E-C. Yang, W. Wernsdorfer, S. Hill, R. S. Edwards, M. Nakano, S. Maccagnano, L. N. Zakharov, A. L. Rheingold, G. Christou and D. N. Hendrickson, *Polyhedron,* 2003, **22**, 1727; (b) E. del Barco, A. D. Kent, E-C. Yang and D. N. Hendrickson, *Polyhedron,* 2005, **24**, 2695; (c) D. N. Hendrickson, E-C. Yang, R. M. Isidro, C. Kirman, J. Lawrence, R. S. Edwards, S. Hill, A. Yamaguchi, H. Ishimoto, W. Wernsdorfer, C. Ramsey, N. Dalal and M. M. Olmstead, *Polyhedron,* 2005, **24**, 2280; (d) E.-C. Yang, W. Wernsdorfer, L. N. Zakharov, Y. Karaki, A. Yamaguchi, R. M. Isidro, G.-D. Lu, S. A. Wilson, A. L. Rheingold, H. Ishimoto and D. N. Hendrickson, *Inorg. Chem.,* 2006, **45**, 529; (e) J. Lawrence, E-C. Yang, R. Edwards, M. M. Olmstead, C. Ramsey, N. S. Dalal, P. K. Gantzel, S. Hill and D. N. Hendrickson, *Inorg. Chem.,* 2008, **47**, 1965; For the first non-cubane-type Ni(II) SMM see: (f) C. Cadiou, M. Murrie, C. Paulsen, V. Villar, W. Wernsdorfer and R. E. P. Winpenny, *Chem. Commun.,* 2001, 2666.

19 (a) M. A. El-Sayed, *Polyhedron,* 1992, **11**, 1261; (b) G. Z. Cai, G. Davies, A. El-Toukhy, T. R. Gilbert and M. Henary, *Inorg. Chem.,* 1985, **24**, 1701; (c) A. El-Toukhy, G. Z. Cai, G. Davies, T. R. Gilbert, K. D. Onan and M. Veidis, *J. Am. Chem. Soc.,* 1984, **106**, 4596; (d) L. L. de Oliveira, R. R. Campedelli, A. L. Bergamo, A. H. D. P. dos Santos and O. L. Casagrande, *J. Braz. Chem. Soc.,* 2010, **21**, 1318.

20 (a) B. N. Figgs and M. A. Hitchman, *Ligand-Field Theory and its Applications*, Wiley-VCH, New York, 2000; (b) C. J. Ballhausen, *Introduction to Ligand-Field Theory*, McGraw-Hill, New York, 1962; (c) J. S. Griffith, *The Theory of Transition-Metal Ions*, Cambridge University Press, Cambridge, 1961.

21 O. Kahn, *Molecular Magnetism*, VCH, Weinheim, 1993.

22 (a) E. König and S. Kremer, *Magnetism Diagrams for Transition Metal Ions*, Plenum Press, New York, 1979; (b) A. B. P. Lever, *Inorganic Electronic Spectroscopy*, Elsevier, Amsterdam, 1984.

23 (a) M. E. Lines, *J. Chem. Phys.,* 1971, **55**, 2977; (b) H. Lueken, P. Hannibal, K. Handrick and J. Schmitz, *Z. Kristallogr.,* 1989, **186**, 185.

24 (a) G. Aromi, S. M. J. Aubin, M. A. Bolcar, G. Christou, H. J. Eppley, K. Folting, D. N. Hendrickson, J. C. Huffman, R. C. Squire, H. L. Tsai, S. Wang and M. W. Wemple, *Polyhedron,* 1998, **17**, 3005; (b) M. Fujita, A. Powell and C. Creutz, Eds. *From the molecular to the nanoscale: Synthesis, structure, and properties;* Elsevier Ltd.: Oxford, U.K., 2004, Vol. **7**; (c) See also special issues of *J. Mater. Chem.,* 2006, **16**, 2501; *Chem. Soc. Rev.,* 2011, **40**, 3053; *Dalton Trans.,* 2012, **44**, 13555 and the ACS virtual issue on "Quantum Molecular Magnets", Ed. K. R. Dunbar, *Inorg. Chem*., 2012, **51**, 12055.

25 (a) R. Sessoli, D. Gatteschi, A. Caneschi and M. A. Novak, *Nature,* 1993, **365**, 141; (b) D. Gatteschi and R. Sessoli, *Angew. Chem., Int. Ed.,* 2003, **42**, 268; (c) R. E. P. Winpenny, *Adv. Inorg. Chem.* 2001, **52**, 1; (d) G. Aromí and E. K. Brechin, *Struct. Bonding,* 2006, **122**, 1; (e) A. M. Ako, I. J. Hewitt, V. Mereacre, R. Clérac, W. Wernsdorfer, C. E. Anson and A. K. Powell, *Angew. Chem. Int. Ed.,* 2006, **45**, 4926; (f) T. C. Stamatatos and G. Christou, *Inorg. Chem.*, 2009, **48**, 3308; (g) R. Sessoli and A. K. Powell, *Coord. Chem. Rev.,* 2009, **253**, 2328; (h) T. Taguchi, W. Wernsdorfer, K. A. Abboud and G. Christou, *Inorg. Chem.,* 2010, **49**, 199; (i) C. Lampropoulos, G. Redler, S. Data, K. A. Abboud, S. Hill and G. Christou, *Inorg. Chem.,* 2010, **49**, 1325; (j) C. Papatriantafyllopoulou, W. Wernsdorfer, K. A. Abboud and G. Christou, *Inorg. Chem*., 2011, **50**, 421.

26 K. S. Cole and R. H. Cole, *J. Chem. Phys.,* 1941, **9**, 341.

27 (a) S. Grimme, J. Antony, S. Ehrlich and H. Krieg, *J. Chem. Phys.,* 2010, **132**, 154104; (b) S. Grimme, *WIREs Comput. Mol. Sci.,* 2011, **1**, 211; (c) S. Grimme, *Chem. Eur. J.,* 2012, **18**, 9955.

28 For review about high-spin molecules, see: H. Oshio and M. Nakano, *Chem. Eur. J.,* 2005, **11**, 5178.

29 R. Boča, *Coord. Chem. Rev.,* 2004, **248**, 757.

30 (a) L. A. Zotti, E. Leary, M. Soriano, J. C. Cuevas and J. J. Palacios, *J. Am. Chem. Soc.,* 2013, **135**, 2052; (b) Y. Kitagawa, T. Matsui, Y. Nakanishi, Y. Shigeta, T. Kawakami, M. Okumura and K. Yamaguchi, *Dalton Trans.,* 2013, **42**, 16200.

31 D. E. Wheeler and J. K. McCusker, *Inorg. Chem.,* 1998, **37**, 2296.

32 See, e.g.: J. Tercero, E. Ruiz, S. Alvarez, A. Rodríguez-Fortea and P. Alemany, *J. Mater. Chem.,* 2006, **16**, 2729.

33 R. J. Errington, *Advanced Practical Inorganic and Metalorganic Chemistry*, CRC press, 1997, p. 246.

34 Bruker-Nonius, *Kappa CCD Reference Manual,* Nonius BV, The Netherlands, 1998.

35 G. M. Sheldrick, *Acta Cryst.,* 2008, **A64**, 112.

36 A. L. Spek, *J. Appl. Crystallogr.,* 2003, **36**, 7.

37 ADF2010.01, SCM, Theoretical Chemistry, Vrije Universiteit, Amsterdam, The Netherlands, http://www.scm.com. E. J. Baerends, J. Autschbach, A. Bérces, C. Bo, P. M. Boerrigter, L. Cavallo, D. P. Chong, L. Deng, R. M. Dickson, D. E. Ellis, L. Fan, T. H. Fischer, C. Fonseca Guerra, S. J. A. van Gisbergen, J. A. Groeneveld, O. V. Gritsenko, M. Grüning, F. E. Harris, P. van den Hoek, H. Jacobsen, G. van Kessel, F. Kootstra, E. van Lenthe, D. A. McCormack, V. P. Osinga, S. Patchkovskii, P. H. T. Philipsen, D. Post, C. C. Pye, W. Ravenek, P. Ros, P. R. T. Schipper, G. Schreckenbach, J. G. Snijders, M. Solà, M. Swart, D. Swerhone, G. te Velde, P. Vernooijs, L.

Versluis, O. Visser, E. van Wezenbeek, G. Wiesenekker, S. K. Wolff, T. K. Woo, T. Ziegler.

38 (a) G. te Velde, F. M. Bickelhaupt, E. J. Baerends, C. Fonseca Guerra, S. J. A. van Gisbergen, J. G. Snijders and T. Ziegler, *J. Comput. Chem.,* 2001, **22**, 931; (b) C. Fonseca Guerra, O. Visser, J. G. Snijders, G. te Velde and E. J. Baerends, In *Methods and Techniques for Computational Chemistry* (Eds.: E. Clementi, G. Corongiu), STEF: Cagliari, 1995, 305; (c) E. J. Baerends, D. E. Ellis and P. Ros, *Chem. Phys.,* 1973, **2**, 41; (d) E. J. Baerends and P. Ros, *Chem. Phys.,* 1975, **8**, 412; (e) E. J. Baerends and P. Ros, *Int. J. Quantum Chem. Symp.,* 1978, **12**, 169; (f) C. Fonseca Guerra, J. G. Snijders, G. te Velde and E. J. Baerends, *Theor. Chem. Acc.,* 1998, **99**, 391; (g) P. M. Boerrigter, G. te Velde and E. J. Baerends, *Int. J. Quantum Chem.,* 1988, **33**, 87; (h) G. te Velde and E. J. Baerends, *J. Comp. Phys.,* 1992, **99**, 84; (i) E. van Lenthe and E. J. Baerends, *J. Comput. Chem.,* 2003, **24**, 1142; (j) J. Krijn and E. J. Baerends, *Fit-Functions in the HFS-Method; Internal Report (in Dutch)*, Vrije Universiteit, Amsterdam, 1984; (k) L. Versluis and T. Ziegler, *J. Chem. Phys.,* 1988, **88**, 322; (l) J. C. Slater, *Quantum Theory of Molecules and Solids,* Vol. **4**, McGraw-Hill, New York, 1974; (m) A. D. Becke, *J. Chem. Phys.,* 1986, **84**, 4524; (n) A. D. Becke, *Phys. Rev. A,* 1988, **38**, 3098; (o) S. H. Vosko, L. Wilk and M. Nusair, *Can. J. Phys.,* 1980, **58**, 1200; (p) J. P. Perdew, *Phys. Rev. B*, 1986, **33**, 8822 (Erratum: *Phys. Rev. B,* 1986, **34**, 7406); (q) L. Fan and T. Ziegler, *J. Chem. Phys.,* 1991, **94**, 6057.

39 M. Swart and J. G. Snijders, *Theor. Chem. Acc.,* 2003, **110**, 34 (Erratum: *Theor. Chem. Acc.,* 2004, **111**, 56).

40 (a) S. Grimme, *J. Comput. Chem.,* 2006, **27**, 1787; (b) S. Grimme, J. Antony, S. Ehrlich and H. Krieg, *J. Chem. Phys.,* 2010, **132**, 154104; See also: (c) S. Grimme, *J. Comput. Chem.,* 2004, **25**, 1463; (d) S. Grimme, *J. Comput. Chem*., 2006, **27**, 1787; (e) S. Grimme, J. Antony, T. Schwabe and C. Muck-Lichtenfeld, *Org. Biomol. Chem*., 2007, **5**, 741; (f) S. Grimme, J. Anthony, S. Ehrlich and H. Krieg, *J. Chem. Phys*., 2010, **132**, 154104; (g) S. Grimme, R. Huenerbein and S. Ehrlich, *ChemPhysChem,* 2011, **12**, 1258.

41 For the use of BP86-D3 see, e.g.: (a) J. M. Ruiz, C. Fonseca Guerra, F. M. Bickelhaupt, *J. Phys. Chem. A,* 2011, **115**, 8310; (b) A. Banerjee, F. S. Raad, N. Vankova, B. S. Bassil, T. Heine and U. Kortz, *Inorg. Chem.,* 2011, **50**, 11667; (c) W. Ames, D. A. Pantazis, V. Krewald, N. Cox, J. Messinger, W. Lubitz and F. Neese, *J. Am. Chem. Soc.,* 2011, **133**, 19743.

42 E. van Lenthe, E. J. Baerends and J. G. Snijders, *J. Chem. Phys*., 1994, **101**, 9783.

43 (a) A. Klamt and G. Schüürmann, *J. Chem. Soc. Perkin Trans.,* 1993, **2**, 799; (b) A. Klamt, *J. Phys. Chem.,* 1995, **99**, 2224; (c) A. Klamt and V. Jones, *J. Chem. Phys.,* 1996, **105**, 9972.

44 (a) A. Bérces, R. M. Dickson, L. Fan, H. Jacobsen, D. Swerhone and T. Ziegler, *Comput. Phys. Commun.,* 1997, **100**, 247; (b) H. Jacobsen, A. Bérces, D. Swerhone and T. Ziegler, *Comput. Phys. Commun.,* 1997, **100**, 263; (c) S. K. Wolff, *Int. J. Quantum Chem.,* 2005, **104**, 645.

45 (a) M. Ernzerhof and G. E. Scuseria, *J. Chem. Phys.,* 1999, **110**, 5029; (b) C. Adamo and V. Barone, *J. Chem. Phys.,* 1999, **110**, 6158.

46 P. J. Stephens, F. J. Devlin, C. F. Chabalowski and M. J. Frisch, *J. Phys. Chem.,* 1994, **98**, 11623.

47 F. Neese, *ORCA - An Ab Initio, Density Functional and Semiempirical Program Package, Version 2.9.0*, Germany.

48 M. R. Pederson and S. N. Khanna, *Phys. Rev. B*. 1999, **60**, 9566.

TOC Synopsis

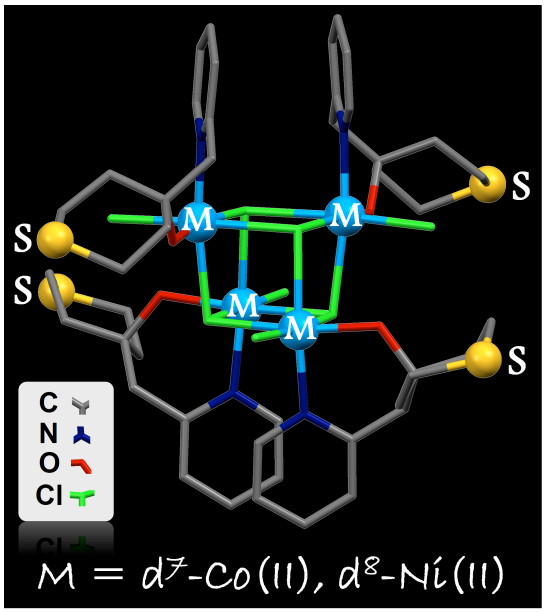

The magnetochemistry of *iso*structural M_4Cl_4 cubane-type complexes $[M(\mu_3\text{-Cl})Cl(\mathbf{HL{\cdot}S})]_4$ (**1**: M = Co and **2**: M = Ni) supported by the new thioether-containing pyridyl-alcohol ligand **HL·S** is strongly influenced by the nature of the transition metal ions, ligand field effects, and magnetic anisotropy characteristics, resulting in SMM behaviour for **2** but not for **1**.